RSC Advances

PAPER

View Article Online
View Journal | View Issue

Cite this: *RSC Adv.*, 2015, **5**, 73133

Repeated self-healing of nano and micro scale cracks in epoxy based composites by tri-axial electrospun fibers including different healing agents†

Jamal Seyyed Monfared Zanjani,[a] Burcu Saner Okan,*[b] Ilse Letofsky-Papst,[c] Yusuf Menceloglu[a] and Mehmet Yildiz*[a]

Received 3rd August 2015
Accepted 19th August 2015

DOI: 10.1039/c5ra15483a

www.rsc.org/advances

Multi-walled healing fibers with a novel architecture are fabricated through a direct, one-step tri-axial electrospinning process to encapsulate different healing agents inside the fibers with two distinct protective walls. Self healing systems based on ring opening metathesis polymerization (ROMP) and an amine–epoxy reaction are redesigned by utilizing these tri-axial fibers. In ROMP, Grubbs' catalysts are integrated in the outer wall of the fibers instead of the composite matrix to reduce the catalyst amount and prevent its deactivation during composite production. In the amine–epoxy healing system, epoxy resin and an amine-based curing agent are encapsulated separately by a multi-axial electrospinning. The presence of an extra layer facilitates the encapsulation of amine based healing agents with a highly active nature and extends the efficiency and life-time of the healing functionality. These new self-healing designs provide repeated self healing ability to preserve the mechanical properties of the composite by repairing micro and nano scale cracks under high loadings.

Introduction

Embedding reinforcing fibers into the polymeric matrix is the most common way to improve the structural performance (*i.e.*, specific strength and stiffness, among others) of polymeric materials.[1] However, the reinforced polymeric materials (composites in general terms) are inherently susceptible to crack initiation and subsequent growth under external loads due to their heterogeneous structure, which unavoidably leads to a gradual degradation in mechanical properties of the composites as a function of time.[2,3] In order to circumvent this issue, it would be a prudent approach to use reinforcing fibers with healing/repairing agent(s) in composite materials.[4] Reinforcing fibers with an healing functionality can improve the mechanical properties of composites, prolong their effective lifetime and expand their capabilities for more advance applications.[5] Inspired by autonomous healing of wounds in living biological systems, scientist and engineers have been in constant search of methods to develop smart materials with self healing capability.[6] One practical approach is based on the delivery of encapsulated liquid agent into fractured areas whereby the mechanical properties of the damaged polymeric material can be partially or fully restored by repairing micro cracks.[7,8] In literature, one may uncover several studies with focus of developing better encapsulation techniques which brings about improved self-healing efficiency of polymeric composite.[9] In one of these studies, Motuku *et al.*[10] demonstrated that the lower impact energy of hollow glass fiber facilitated the rupture of healing fibers and consequently the release of healing agent in micro- and macro-cracks in comparison to copper and aluminum hollow fibers. It should be noted that the presence of these hollow glass fibers in matrix reduces the initial strength of material albeit an increase in damage tolerance and residual strength of composite structure.[11] In addition, filling diminutive hollowness of fibers with a healing agent is not a trivial step in the production of these kinds of self-healing fibers.[4,12,13] At this point, core–shell or co-axial electrospinning can be deemed as a promising, versatile, one-step, and efficient technique to encapsulate a broad range of materials in multi-walled nano/micro fibers with a controllable diameter, wall thickness, mechanical properties and surface morphology.[14] In this process, an electric potential difference is created between a collector and a concentric metallic nozzle which host polymeric solution as a shell material in the outer tube and a liquid to be encapsulated as a core material in the

[a]*Faculty of Engineering and Natural Sciences, Advanced Composites and Polymer Processing Laboratory (AC2PL), Sabanci University, Tuzla, Istanbul 34956, Turkey. E-mail: meyildiz@sabanciuniv.edu*

[b]*Sabanci University Nanotechnology Research and Application Center, SUNUM, Tuzla, Istanbul 34956, Turkey. E-mail: bsanerokan@sabanciuniv.edu*

[c]*Institute for Electron Microscopy, Graz University of Technology, Steyrergasse 17, A-8010, Graz, Austria*

† Electronic supplementary information (ESI) available. See DOI: 10.1039/c5ra15483a

inner tube. Due to the electrohydrodynamic forces, both encapsulant and the core fluids are coaxially extruded though the tip of the nozzle in the form of a jet moving towards the collector while undergoing bending instabilities, whipping motions and diameter reduction, and reach at the collector as co-axial electrospun fibers with encapsulated core liquid and with a diameter ranging from several nanometers to micrometers.[15] In the core–shell electrospinning, the outer shell is required to be a polymeric solution with viscoelastic properties, but the core solution can be either viscoelastic or Newtonian liquids.[16] The encapsulation by co-axial electrospinning technique is a physical phenomenon and relies on the physical forces and interactions which eliminate the need for chemically complex and expensive encapsulation methods, and brings a new insight into the design and chemistry of self-healing fibers.[17,18] Park *et al.*[19] encapsulated polysiloxane-based healing agents into a poly(vinyl-pyrrolidone) coaxial electrospun beads with the diameters of 2 to 10 μm, which were obtained randomly on electrospun nano-fibers. Moreover, Mitchell *et al.*[20] obtained beads with the average diameter of 1.97 μm on the nano fibers with the diameter of 235 nm during coaxial electrospinning of poly(vinyl alcohol) as a shell and epoxy resin as a healing agent.

The critical point in fiber based healing systems is continuous and repetitive release of healing agent into the damaged area, but fibers including beads do not provide this continuity and thus uniformity in fiber structure carries a significant importance to increase self-healing degree. Therefore, Sinha-Ray *et al.*[14] employed three different techniques (*i.e.*, co-electrospinning, emulsion electrospinning and emulsion solution blowing) to encapsulate healing agents of dicyclopentadiene (DCPD) and isophorone diisocyanate into vascular network like core shell fibers produced by polyacrylonitrile (PAN) in the diameter range of micrometers. The integration of DCPD encapsulated coaxial electrospun PAN fibers into hybrid multi-scale high-strength carbon fiber/epoxy composites as a self healing interlayer restores the toughness of structure due to the self healing functionality.[21]

The chemistry of vascular based self-healing composite materials directly affects the stability and life-time of monomer during composite manufacturing process, polymerization kinetics, the delivery of healing agents, mechanical properties of the newly formed polymer as well as its compatibility with matrix.[22] However, there are a limited number of self-healing chemistries to initiate the polymerization in the crack area. Ring opening metathesis polymerization (ROMP) is one of the well-known self-healing systems in which bicyclic monomers such as norbornene derivatives release inside the crack and react with the catalyst that is deposited in the matrix through living polymerization in order to recover the mechanical properties of composite matrix.[6,23–26] An innovative work in this field was conducted by White *et al.*[6] who introduced ROMP of DCPD monomers in the presence of Grubbs' catalyst as a healing motif in epoxy matrix. In this approach, crack propagation ruptures micro-capsules containing DCPD monomers and then monomers release inside the crack and react with the pre-dispersed Grubbs' catalyst within matrix and a solid, highly cross-linked polymer, is formed by ROMP reaction.

In spite of exceptional properties of DCPD and Grubbs' catalyst as a healing system such as long shelf-life, low viscosity of healing agent as well as good mechanical properties of the resulting polymer,[26] this system suffers from the deactivation of Grubbs' catalyst upon exposure to air[27] and at high temperature,[28] and in the presence of diethylenetriamine which is used as a curing agent of epoxy matrix.[29] As an alternative to DCPD monomer, many efforts have been devoted to the development of self-healing chemistry by using epoxy as a repairing agent which is chemically and physically more compatible to host matrix than DCPD.[30,31] Epoxy resin is considered as a promising candidate to reduce the cost of self-healing material production and improve self-healing efficiency by increasing the compatibility with the matrix. Yin *et al.*[30] produced self-healing woven glass fabric/epoxy composites including epoxy-loaded urea formaldehyde microcapsules fabricated by emulsion polymerization and cupper based metal catalysts as a latent hardener embedded in the host matrix. In another work, instead of using a metal catalyst as a hardener, amine solution was filled inside hollow glass bubbles by a vacuum assisted method and these capsules together with microcapsules containing epoxy solution are concurrently integrated into a matrix for the production of self-healing composites.[32,33]

There are only a few published studies on the encapsulation of hardener inside polymeric shells for curing epoxy healing agent thus repairing the damaged area in the matrix.[34,35] To the authors' knowledge, the encapsulation of epoxy and its hardener by multi-axial electrospinning technique and determination of the self-healing degree of composites including these healing agents have not been reported yet. To this end, in the first part of the present study, DCPD as a healing agent is encapsulated inside electrospun fibers constituting two different polymeric layers with dissimilar hydrophilicity, namely, polyacrylamide (PAAm) as an inner layer and polymethyl methacrylate (PMMA) containing metal catalysts as an outer layer. The low affinity between the inner wall polymer and encapsulated healing agent within the core of fibers limits the interaction of healing agent with its surrounding media and decreases the diffusion rate of healing agent through the wall of fiber hence extending the efficiency and lifetime of healing functionality of fibers. Moreover, the presence of inner layer, PAAm, prevents the direct contact between the catalysts and DCPD healing agent in core part of fiber. The integration of catalyst particles in outer layer of fibers instead of the composite matrix reduces the required amount of this expensive and toxic catalyst, prevents the deactivation of catalyst during the manufacturing process and its service life and more importantly, guarantees the presence of catalyst in the crack area to initiate the polymerization of self-healing agent released from fibers. In the second part of this work, epoxy resin and amine-based curing agent are encapsulated separately by multi-axial electrospinning and these produced fibers are embedded into composite matrix to measure their self-healing efficiency. The viscosity of epoxy resin inside multi-axial fibers is optimized at different diluent ratios for the effective encapsulation and

enhancing self-healing. In addition, the effect of fiber diameter and the type of self-healing agent (DCPD monomer and epoxy resin) on the self-healing properties of the produced composites is investigated by comparing the modulus reduction values by conducting multiple healing cycles.

Experimental

Materials

Materials used are methyl methacrylate (SAFC, 98.5%), styrene (SAFC, 99%), glycidyl methacrylate (Aldrich, 97%), azobisisobutyronitrile (AIBN, Fluka, 98%), acrylamide (Sigma, 99%), *N*,*N*-dimethyl formamide (DMF, Sigma-Aldrich, 99%), methanol (Sigma-Aldrich, 99.7%), tetrahydrofuran (THF, Merck, 99%), ethyl acetate (EA, Sigma-Aldrich, 99.5%), dicyclopentadiene (DCPD, Merck), Grubbs' catalyst (2nd Generation, Aldrich), acetone (Aldrich, 99.5%), Disperse Red 1 (Fluka), LY 564 resin, and Hardener XB 3403 (Huntsman).

Synthesis of layer materials

Polymethyl methacrylate (PMMA), polystyrene (PS) and poly(glycidyl methacrylate-*co*-styrene) as outer layer material of fibers was synthesized by free radical polymerization of vinyl monomers (30 ml) in the presence of AIBN (1 g) as a radical initiator in the medium of THF (50 ml) at 65 °C. Polymerization reaction was carried out for 4 h and then the reaction mixture was precipitated in cold methanol and dried for 12 h in a vacuum oven at 50 °C. Polyacrylamide (PAAm) as a hydrophilic polymer and inner layer material was synthesized by dispersion polymerization of acrylamide monomer (30 g) in methanol (100 ml) by using AIBN (1 g) as an initiator at 65 °C. Separation of polymer from methanol and unreacted monomer was done by vacuum filtration and washing twice with methanol and drying for 12 h in a vacuum oven at 40 °C.

Multi-axial electrospinning

Tri-axial fibers are produced at ambient room conditions by using a multi-axial electrospinning set-up purchased from Yflow Company with a custom-made tri-axial nozzle. Scheme 1 shows the schematic representation of multi-axial electrospinning process that can produce double walled electrospun fibers with a healing agent as a core material. All fibers were electrospun with a nozzle to collector distance of 7 cm by tuning the applied voltage in the range of 5 kV to 30 kV. Solutions are loaded independently into the syringes connected to concentric nozzles, and the flow rate of each layer is controlled by separate pumps. The flow rates of solutions for the outer and inner layers and the core are 20 μl min^{-1}, 15 μl min^{-1} and 10 μl min^{-1}, respectively.

Fabrication of fiber reinforced epoxy composites

Classical molding technique is utilized to prepare fiber reinforced composites. In this method, 2 wt% multiaxial electrospun hollow fibers and healing fibers with the same hollow fiber content (*i.e.*, excluding the weight of the healing agent) were uniformly laid down into a Teflon mold and then impregnated by the mixture of degassed resin and hardener system. Subsequently, the mold is placed in a vacuum oven to remove entrapped air bubbles and to cure the resin–hardener mixture at 70 °C for 5 days. Electrospun fiber reinforced specimens for three point bending tests have the dimensions of 100 × 14 × 3 mm.

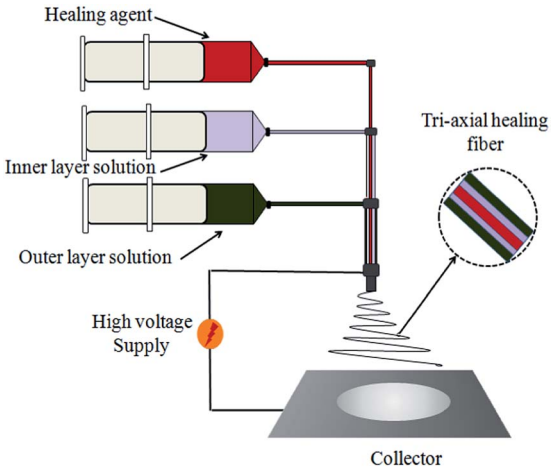

Scheme 1 A schematic representation for the multi-axial electrospinning set-up.

Characterization

The properties of polymers used as layers of electrospun fibers were characterized in detail using Nuclear Magnetic Resonance (NMR) for chemical structure, Gel Permeation Chromatography (GPC) for molecular weight and polydispersity index, Differential Scanning Calorimeter (DSC) for determining glass transition temperature and Thermal Gravimetric Analyzer (TGA) for thermal decomposition in our previous studies[36,37] and hence were not given here again to avoid redundancy. The functional groups of polymers and fibers were analyzed by Netzsch Fourier Transform Infrared Spectroscopy (FTIR). The surface morphologies of fibers were analyzed by a Leo Supra 35VP Field Emission Scanning Electron Microscope (SEM) and JEOL 2100 Lab6 High Resolution Transmission Electron Microscopy (TEM). Rheological analyses were performed by using a rotational rheometer (Malvern Bohlin CVO). Gel contents of the cured neat specimens were determined by Soxhlet extraction for 24 h using THF. The extracted samples were vacuum dried at 80 °C until achieving a constant weight. Three point flexural tests on composite specimens were performed by using ZWICK Proline 100 Universal Test Machine (UTM) with 10 kN load cell using a constant cross-head speed of 1 mm min^{-1}.

Results and discussion

Fabrication of multi-walled healing fiber

In our previous study, we have performed a systematical optimization study to produce tri-axial hollow electrospun fibers with tunable fiber diameters and surface morphologies[36] and demonstrated that the use of solvents with a higher vapor pressure (*i.e.*, THF) resulted in fibers with larger diameters

whereas solvents with a lower vapor pressure (*i.e.*, EA and DMF) led to fibers with smaller diameters. In the present study, for self-healing application, healing agent encapsulated tri-axial fibers having different fiber diameters and surface morphologies were fabricated following the systematic in given.[36] This method enables the encapsulation of different types of healing agents within electrospun fibers with different outer wall materials and tailorable interfacial properties whereby the fabrication of healing fibers with a novel architecture becomes possible. Self-healing mechanisms of tri-axial fibers in composite matrix are investigated by applying two different chemistries: ring opening metathesis polymerization (ROMP) and amine–epoxy reaction.

Fabrication of self-healing multi-walled fibers based on ROMP

In literature, it was reported that the healing system based on the ring-opening metathesis polymerization (ROMP) of DCPD monomer with a very low viscosity and a low surface energy catalyzed by Grubbs' catalyst repairs damaged areas through restoring the mechanical properties of composite matrix and consequently fulfills requirements expected by an ideal self-healing system.[38,39] In order to obtain multi-axial fibers with healing functionality, DCPD is encapsulated as a core material inside the tri-axial fibers having different outer layer polymers that are compatible with epoxy matrix, and a hydrophilic middle layer that provides an inert media for DCPD monomer inside the fibers. In literature, metal-based catalytic curing agents (*i.e.*, solid-phase reagents) such as Grubbs' catalyst are commonly mixed with epoxy resin to act as a self-healing agent initiator and promote ring-opening polymerization of encapsulated DCPD.[40] However, Grubbs' catalyst is not cost-effective for the production of a large-scale self-healing composite. Therefore, in the present study, following an alternative approach, catalyst particles were dispersed into the outer layer polymer of electrospun fibers before the electrospinning process in order to minimize the use of catalyst in the composite structure as well as provide a direct contact of catalyst with monomer in the nearest region of the crack. The presence of organic groups in the structure of catalyst makes this organometallic catalyst highly compatible and soluble within several solvents used for the preparation of fibers outer layer. Once the catalyst powder is dissolved in the solvent, it acquires molecular scale thereby being homogeneously distributed in the outer layer of tri-axial fibers. This reduces the catalyst amount used in the preparation of self-healing composite and thus offers a cost effective production. Fig. 1 exhibits SEM images of as received Grubbs' catalyst at different magnifications.

PMMA, PS and poly(glycidyl methacrylate-*co*-styrene) are chosen as outer wall polymers of electrospun fibers due to their interfacial compatibility with epoxy matrix. The interfacial interactions between outer wall of electrospun fiber and polymer matrix play a critical role in load transfer from matrix to the fibers and thus improve the mechanical properties of composite.[41] In our previous work, we have shown that the integration of multi-walled hollow fibers with outer layer of

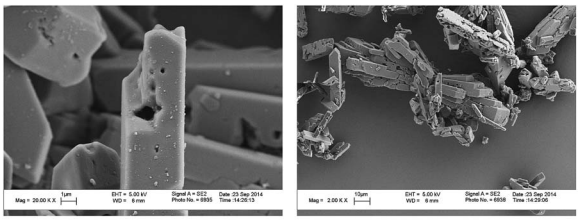

Fig. 1 (a) and (b) SEM images of as received Grubbs' catalyst at different magnifications.

PMMA and the diameter of 100 nm into epoxy matrix improves the flexural modulus by 28%, and flexural strength by 21%.[37] Mechanical improvement in electrospun fiber reinforced epoxy specimens can be explained by the interpenetration of partially dissolved PMMA chains into epoxy and hardener mixture, resulting in the entanglement of linear PMMA chains with the cross-linked matrix network and thus the formation of semi interpenetrating polymer network (semi-IPN) structure which improves load transfer between matrix and electrospun fibers.[37] Therefore, self-healing functionality is selectively added to these electrospun fibers through encapsulating the healing agent therein by adjusting fiber diameter by using different solvents. Fig. 2a exhibits SEM image of PMMA/PAAm/DCPD tri-axial electrospun fibers with diameters over 2 μm which are produced using PMMA solution in THF as an outer wall and PAAm solution in water as a middle wall. Similarly, SEM images given in Fig. 2b and c present PMMA/PAAm/DCPD tri-axial fibers that are fabricated using PMMA solution in EA and DMF as outer wall thereby bring about fibers with diameters of 1 μm and 200 nm, respectively. Healing fibers with larger diameters are expected to contain higher amount of healing agent per unit length of fibers in comparison to that with lower diameter. However, given that the flow rate ratio is kept constant for all experiments, the amount of healing agent in fibers with different diameters is the same per weight unit of fibers. All SEM images in Fig. 2 reveal that PMMA as the outer wall covers the interior layer uniformly and continuous fibers without any bead formation are successfully obtained. Furthermore, the solvent type directly affects the surface morphology and porosity of the fibers by due to the thermodynamic instabilities and associated phase separation during the electrospinning process.

In the course of obtaining an ideal fiber morphology containing DCPD monomer, PS and poly(glycidyl methacrylate-*co*-styrene) polymers were also used as outer layers of tri-axial fibers. Fig. 3a exhibits SEM images of PS/PAAm/DCPD tri-axial fibers and the breakage area of this fiber and middle layer are seen clearly that confirms the formation of multi-layer fiber morphology. Fig. 3b represents poly(glycidyl methacrylate-*co*-styrene)/PAAm/DCPD tri-axial fibers fabricated using an outer layer solution prepared in EA and with the diameter of around 1 μm.

To study the self healing efficiency of multi-walled fibers with encapsulated healing agent in a host material, epoxy resin system is reinforced by multi-walled fibers with and without encapsulated healing agent. To ensure that both fiber types

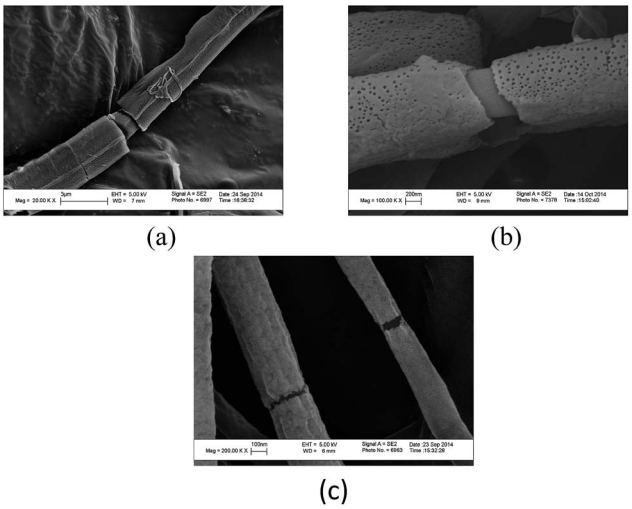

Fig. 2 SEM images of PMMA/PAAm/DCPD tri-axial healing fibers fabricated utilizing different outer wall solvents (a) THF, (b) EA and (c) DMF.

have similar influence on the matrix in terms of crack formation due to their presence, their diameters are controlled to be as uniform as possible. Fig. 4a and b yield multi-walled hollow fibers of PMMA/PAAm with the outer wall material's solution prepared in DMF and EA, respectively. It is seen that the morphology and diameter of these fibers are very similar to the fibers including DCPD shown in Fig. 2b and c, indicating that the encapsulation of DCPD does not affect the fiber structure. To reveal ordered layer formation in fibers, the morphologies of walls with DCPD monomer were analyzed by TEM technique. Fig. 5a and b exhibit PMMA/PAAm/DCPD tri-axial healing fibers prepared using the outer layer solvent of DMF. In order to reveal the presence of the healing agent inside the electrospun fibers, DCPD is initially mixed with a specific dye (Disperse Red 1) which hinders the passage of electrons through fibers thereby resulting in the formation of dark regions in the core of the fibers and the bright regions at the edges corresponding to the polymeric shells on the TEM images. Fig. 5b clearly indicates that the end of the fiber is completely closed by outer layer, which implies that healing agents are completely confined inside fiber structure and only ruptured fibers can release the encapsulated healing agent in the core of the fibers. TEM image of PMMA/PAAm tri-axial hollow fiber prepared by outer layer

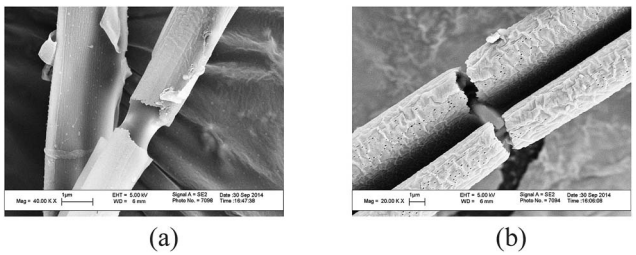

Fig. 3 SEM images of (a) PS/PAAm/DCPD and (b) poly(glycidyl methacrylate-*co*-styrene)/PAAm/DCPD tri-axial healing fibers, which are manufactured using EA as an outer wall solvent.

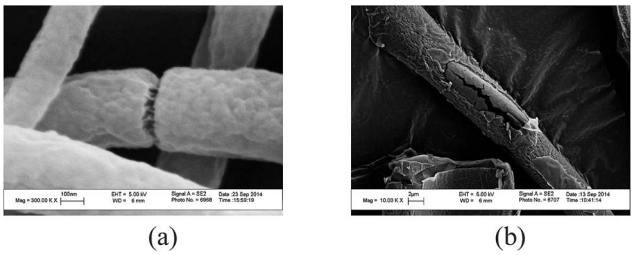

Fig. 4 SEM images of PMMA/PAAm tri-axial hollow electrospun fibers fabricated using different outer wall solvents of (a) DMF, and (b) EA.

solvent of EA in Fig. 5c is an evidence for the presence of two separate walls and empty core of the fiber.

Fig. 6a and b respectively gives images obtained using cathodoluminescence (CL) and coupled secondary electron (SE) for PS/PAAm/DCPD tri-axial healing fibers prepared using DMF as an outer layer solvent. The addition of dye into the healing agent provides an opportunity to have a complete map of healing agent distribution in fibers due to cathodoluminescence effect. In Fig. 6a, brighter fibers contain self-healing agent whereas darker fibers are empty and do not have any dye in the core of fibers, which confirms the presence of healing agent inside the most of electrospun fibers. The morphology of fibers can be clearly seen in Fig. 6b.

Moreover, FTIR analysis was performed to confirm successful encapsulation of healing agent into the multi-walled fibers through identifying the characteristic peak groups of different wall materials and healing agents. Fig. 7a shows FTIR spectra of DCPD, PMMA/PAAm tri-axial hollow fiber and PMMA/PAAm/

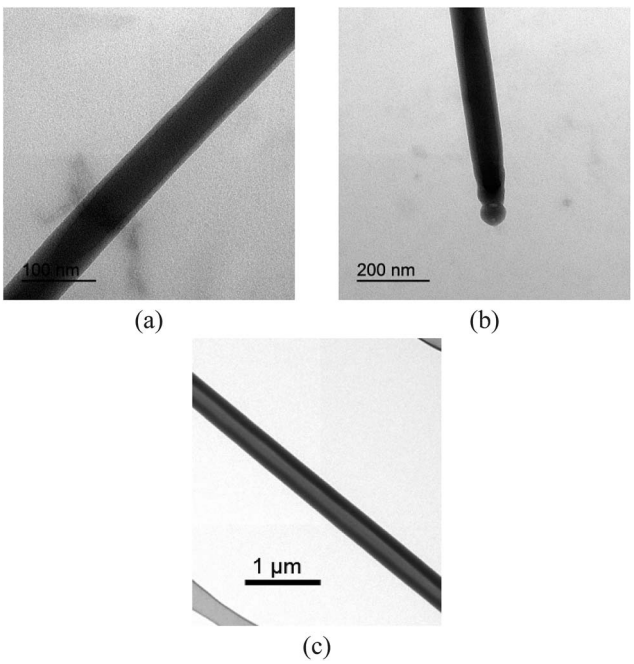

Fig. 5 TEM images of (a and b) PMMA/PAAm/DCPD tri-axial healing fibers fabricated using DMF as an outer layer solvent, and (c) PMMA/PAAm tri-axial hollow fiber electrospun through using EA as an outer layer solvent.

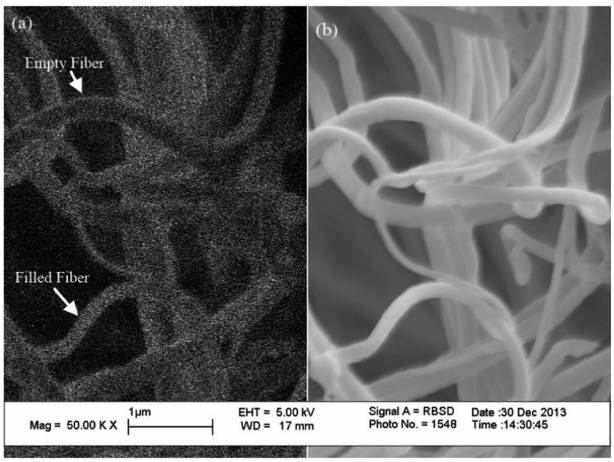

Fig. 6 (a) Cathodoluminescence and (b) secondary electron coupled SEM images of PS/PAAm/DCPD tri-axial electrospun fibers.

DCPD tri-axial fiber. Liquid DCPD monomer prior to encapsulation gives intense and sharp peaks at 725 cm^{-1} and 740 cm^{-1} representing CH=CH bending modes, peak at 3045 cm^{-1} belonging to C=C stretching vibration, peak at 2961 cm^{-1} owing to C–H stretching vibrations, and peak at about 1340 cm^{-1} corresponding to =C–H bending vibration.[42] In the FTIR spectra of electrospun PMMA/PAAm tri-axial hollow fibers in Fig. 7a, the absorption bands at 2950 cm^{-1} and 1745 cm^{-1} belong to C–H and C=O stretchings of PMMA polymer, respectively.[43] The FTIR spectra of PS/PAAm tri-axial hollow fiber and PS/PAAm/DCPD tri-axial fiber in Fig. 7b show absorption bands at 3024 cm^{-1} and 2848 cm^{-1} corresponding to aromatic and aliphatic C–H stretchings of outer wall of PS as well as the peaks at 1600 cm^{-1} and 1492 cm^{-1} assigned to aromatic C=C stretchings of this polymer. FTIR spectrum of poly(glycidyl methacrylate-*co*-styrene) used as an outer wall in Fig. 7c confirms aromatic peaks of styrene and carbonyl group of glycidyl methacrylate at around 1700 cm^{-1}, the peak of oxirane group at 910 cm^{-1} and the peaks of C–O stretching of ester group in the structure of glycidyl methacrylate at 1140 cm^{-1} and 1260 cm^{-1}.[44] In addition, asymmetric and symmetric NH stretching of NH2 at around 3300 cm^{-1} corresponds to PAAm polymer as a middle wall of all fibers.[45] To reiterate, the peaks related to outer and middle wall materials and the characteristic peaks of DCPD monomer are observed in three FTIR spectra of electrospun healing tri-axial fibers, which bespeak a successful encapsulation of healing agents in electrospun fibers with different outer wall materials.

Fabrication of self-healing multi-walled fibers based on amine–epoxy reaction

Due to its reactivity with several curing agents and hardeners at different temperature, excellent adhesion to epoxy matrix, corrosion and chemical resistance, and low curing shrinkage, bisphenol A diglycidyl ether (epoxy resin) can be deemed as versatile healing agent for a wide range of composite materials. However, a direct use of epoxy resin as a healing agent is not practical due to its relatively high viscosity that makes the encapsulation process very hard as well as prevents the flow of the healing agent into the micro-cracks owing to capillarity once the healing fibers or capsules are damaged. To reduce the viscosity and in turn facilitate the encapsulation process, epoxy based healing agent can be diluted in acetone. The excessive addition of acetone into epoxy may reduce the mechanical performance of cured polymer. Hence, it is prudent to keep the amount of acetone used for dilution process at minimum level. In literature, it was reported that mechanical properties of cured epoxy initially diluted using 20 wt% of acetone is basically remained the same as that of cured virgin epoxy resin, which indicates that the appropriately diluted epoxy resin can be easily encapsulated in electrospinning process[46] and be effectively used as self healing agent. In the present study, for easy encapsulation, the viscosity of epoxy based healing agent is also adjusted using acetone. To this end, the viscosity of epoxy resin and acetone mixtures with different ratios was measured by rotational viscometer. Fig. 8 exhibits the normalized viscosity of epoxy–acetone mixtures having different ratios with respect to pure epoxy. It is seen that the addition of 20 wt% acetone into high viscosity epoxy resin causes a dramatic decrease in the viscosity of epoxy; however, further increasing the amount of acetone in the mixture does not change the viscosity much.

Fig. 9 represents SEM images of tri-axial electrospun fibers used as healing reinforcement in epoxy matrix. SEM images of PMMA/PAAm/hardener tri-axial fibers given in Fig. 9a and b show hollowness of fibers after breakage and the release of hardener. Fig. 9c and d exhibit the multi-layered structure of PMMA/PAAm/epoxy tri-axial fibers. In order to start self-healing mechanism in the matrix after the breakage, hardener and epoxy should be encapsulated separately and the fibers should be brittle under high loadings. Fig. 9e and f present TEM images of tri-axial fibers of PMMA/PAAm/hardener and PMMA/PAAm/epoxy with outer layer solvent of EA in which dark regions in the core of the fibers are due to healing agents while the bright regions at the boundaries correspond to the polymeric shells.

FTIR analysis of these tri-axial fibers confirms the presence of encapsulated hardener and epoxy inside the fiber structure. Fig. 10a shows FTIR spectra of hardener, PMMA/PAAm tri-axial hollow fiber and PMMA/PAAm/hardener tri-axial fiber. In tri-axial fiber containing hardener, the peak at 1592 cm^{-1} corresponds to N–H bending vibration and strong peak at 1150 cm^{-1} belongs to C–N stretching that confirms the presence of amine based hardener in the fibers structure.[47] Fig. 10b exhibits the FTIR spectra of epoxy resin, PMMA/PAAm tri-axial hollow fiber and PMMA/PAAm/epoxy tri-axial fibers. In these spectra, the peaks at 815 cm^{-1} and 840 cm^{-1} belonging to oxirane groups verify the presence of epoxy resin in tri-axial fiber structure. After the encapsulation of hardener and epoxy inside tri-axial fiber, the characteristic peaks belonging to PMMA and PAAm are observed in each case and the fingerprints of these polymers are similar to fibers containing DCPD monomer that we discussed in the previous section.

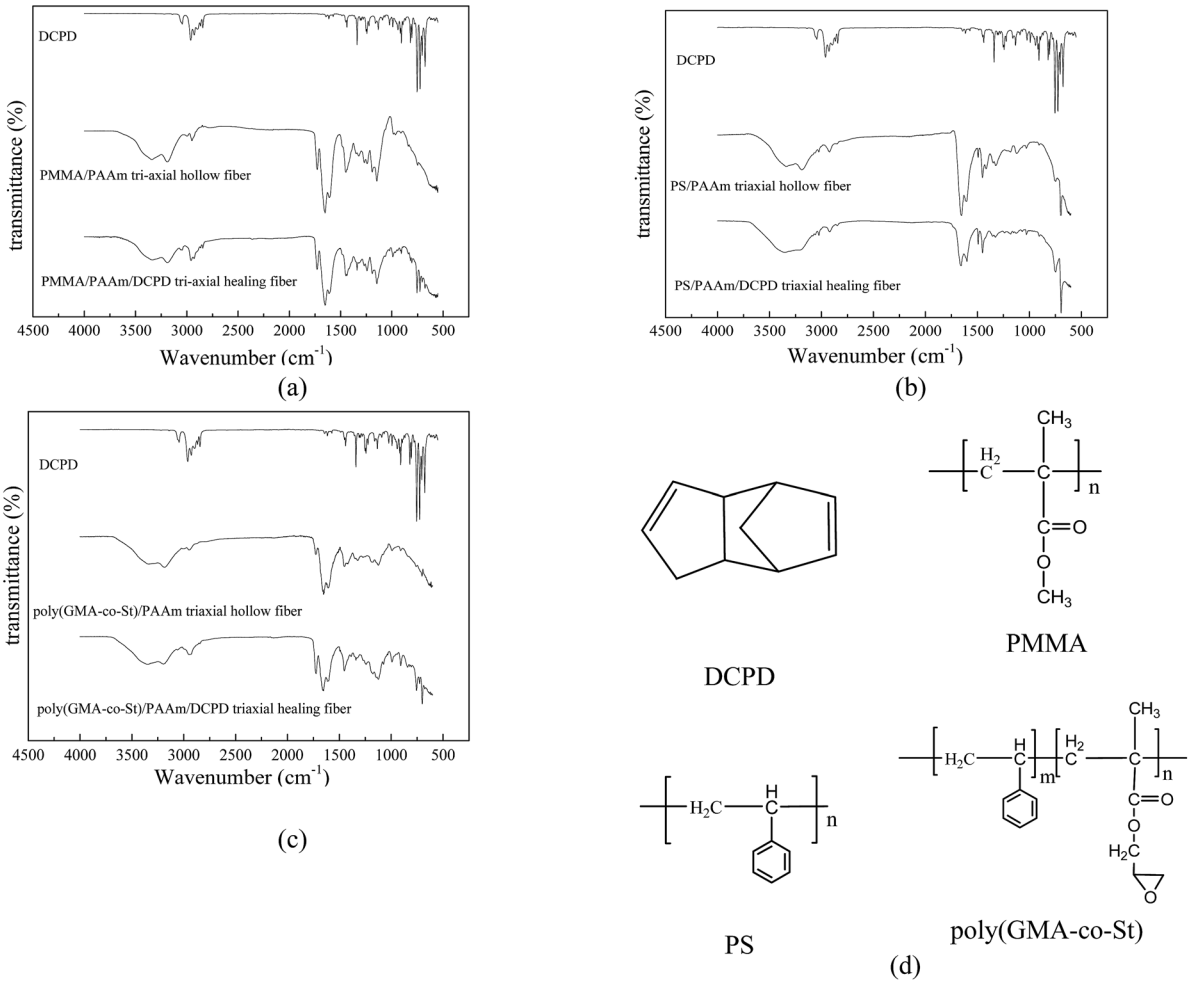

Fig. 7 FTIR spectra of (a) DCPD, PMMA/PAAm tri-axial hollow fiber and PMMA/PAAm/DCPD tri-axial fiber, (b) DCPD, PS/PAAm tri-axial hollow fiber and PS/PAAm/DCPD tri-axial fiber, (c) DCPD, poly(St-*co*-GMA)/PAAm tri-axial hollow fiber and poly(St-*co*-GMA)/PAAm/DCPD tri-axial fiber. (d) The chemical structure of polymers and DCPD.

Determination of the curing state of matrix

In order to eliminate the possible effect of post-curing on the degree of self-healing and obtain optimum curing time for epoxy specimens, gel content of cured neat epoxy specimens were determined as function of curing time through using Soxhlet extraction technique. The value of gel content after extracting uncured oligomers and monomers from structure represents the cross-linking degree of epoxy specimens.[48] In Fig. 11 is plotted the variation of gel content of neat epoxy specimens as a function of curing time at constant curing temperature of 70 °C wherein one can observe that 97% of epoxy and hardener mixture is cured during the first 6 h of curing process and the percentage of cross-linking gets higher with the increasing curing time. However, after certain time of curing at constant temperature, specimens reach at their ultimate curing state and no notable difference is observed in gel content of specimens after this saturation point. Herein, specimens cured for 5 and 6 days show very similar gel content value which corresponds to complete curing.

It is explained that after 5 days of curing at temperature of 70 °C the specimens reach their maximum curing state and the effect of post curing from self healing data can be eliminated completely.

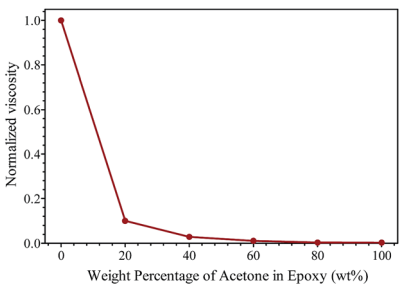

Fig. 8 The change in the viscosity of epoxy resin as a function of volume percentage of acetone.

Evaluation of self-healing efficiency

The usage of tri-axial fiber with epoxy compatible outer layer polymer as a self healing reinforcement in epoxy matrix will

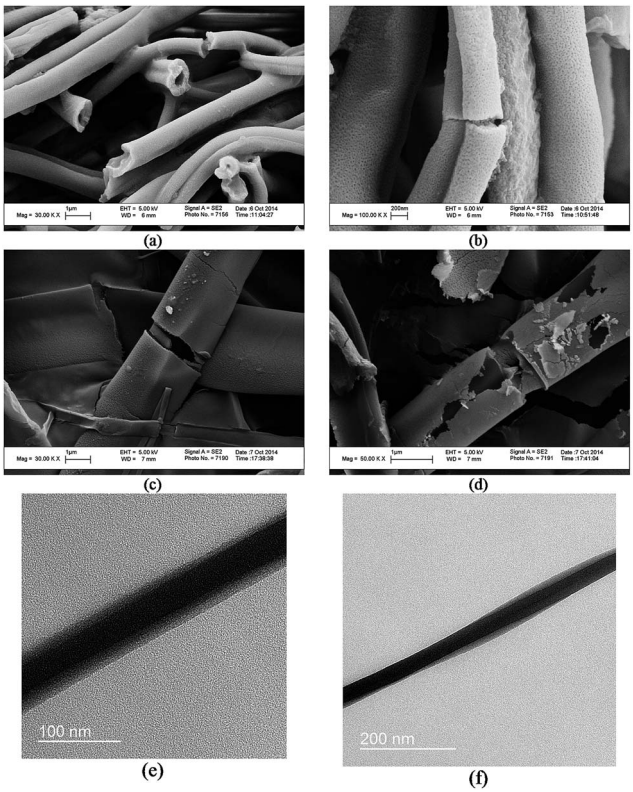

Fig. 9 (a and b) SEM images and (e) TEM image of PMMA/PAAm/hardener tri-axial fiber with 20 wt% PMMA in EA solution as an outer wall, 20 wt% PAAm in water as a middle wall and hardener as a core material (c and d) SEM images and (f) TEM image of PMMA/PAAm/epoxy tri-axial fiber with 20 wt% PMMA in EA solution as an outer wall, 20 wt% PAAm in water as a middle wall and epoxy–acetone 8 : 2 mixture as a core material.

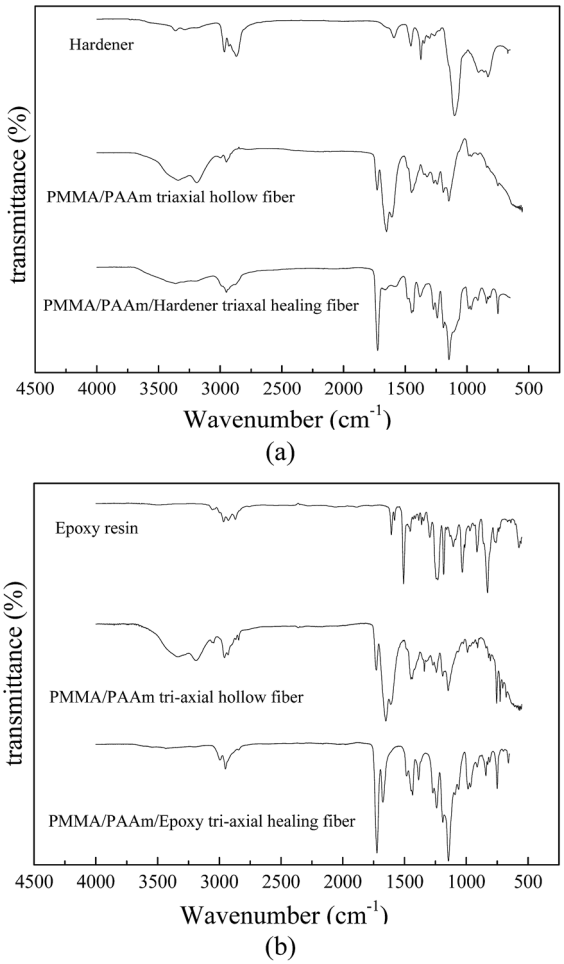

Fig. 10 FTIR spectra of (a) hardener, PMMA/PAAm tri-axial hollow fiber and PMMA/PAAm/hardener tri-axial fiber (b) epoxy resin, PMMA/PAAm tri-axial hollow fiber and PMMA/PAAm/epoxy tri-axial fiber.

expectedly lead to epoxy based composites with enhanced mechanical properties.[37] Therefore, PMMA has been chosen as an outer layer polymer to enhance the interactions between self healing fibers and epoxy matrix. Scheme 2 introduces stages of designed self-healing process schematically.

In order to perform self healing tests, 3-point bending specimens individually reinforced by PMMA/PAAm hollow tri-axial fibers and Grubbs' catalyst dispersed PMMA/PAAm/DCPD tri-axial fibers as well as the couples of PMMA/PAAm/epoxy and PMMA/PAAm/hardener tri-axial fibers were subjected to repeated bending/healing cycles wherein self-healing composite specimens were subjected to 6% flexural strain through utilizing corresponding applied stress and then were kept in oven for 24 h at 70 °C for healing reaction. Fig. 12 exhibits the flexural stress–strain curves of selected specimens reinforced by tri-axial fibers including different healing agents with two different diameters in each cycle. As seen in stress–strain relations, after the strain of 3%, samples begin to have a non-linear behavior or yield, which can be attributed to initiation of cracks inside the composite structure. At this stage, there should be a lot of invisible nano- and micro-cracks forming, coalescing and growing inside the structure under the applied stress. In each repeating cycle, flexural modulus decreases gradually since the size and the number of cracks in the matrix of specimens increase. Fig. 12a demonstrates the flexural stress–strain curves of specimen reinforced by PMMA/PAAm tri-

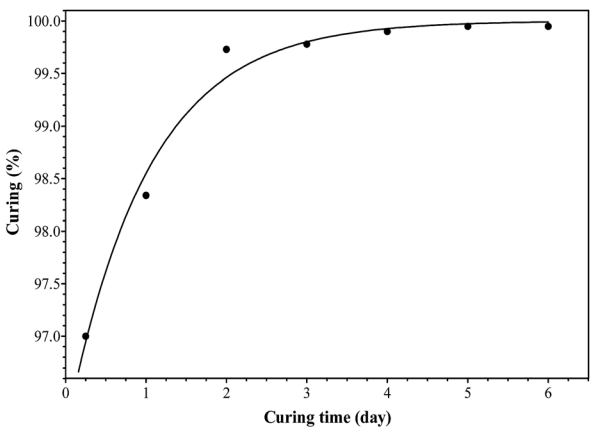

Fig. 11 The variation of gel content of neat epoxy specimens as a function of curing time at constant curing temperature of 70 °C (obtained by Soxhlet extraction).

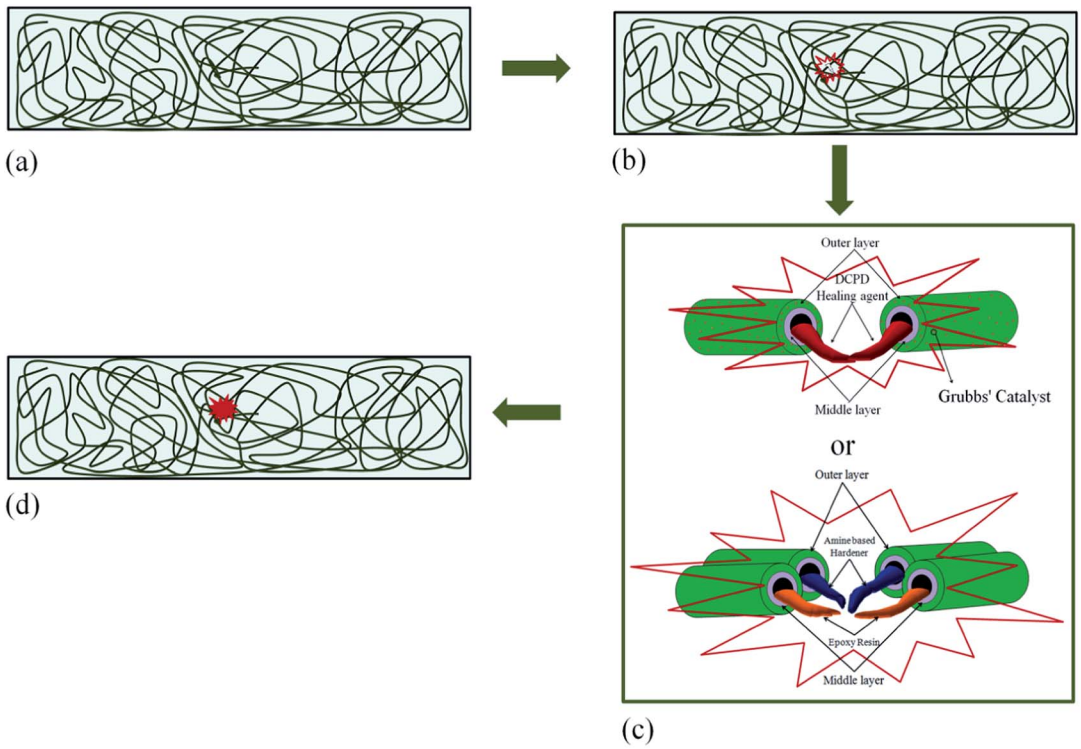

Scheme 2 Schematic representation of self-healing concept, (a) the incorporation of self healing fibers into a polymer matrix, (b) cracks formation within the matrix due to the external load and consequent rupture of healing fibers, (c) the discharge of healing agent into the crack area followed by its polymerization upon getting in contact with either pre-dispersed catalyst in outer layer of fibers or the hardener released along with the healing epoxy, and (d) healing of crack region.

axial hollow fibers with the average fiber diameter of 200 nm while Fig. 12b shows specimen reinforced by PMMA/PAAm/DCPD tri-axial fibers having DCPD healing agent in the core of fiber and Grubbs' catalyst dispersed in the outer wall with the average fiber diameter of 200 nm. In Fig. 12b, the reduction of modulus values of specimen reinforced by tri-axial fibers with self-healing functionality in each cycle is lower than the similar specimens reinforced by hollow fibers. This improvement of modulus in the presence of healing fibers indicates that the DCPD monomer and Grubbs's catalyst react by ring opening polymerization to repair the crack area. Also, Table 1 tabulates the percentages of reduction in the flexural modulus in comparison to first bending cycle of each specimen. Fig. 12c and d show the flexural stress–strain curves of specimens reinforced by PMMA/PAAm tri-axial hollow fiber and PMMA/PAAm/DCPD tri-axial healing fibers with the average fiber diameter of 1 μm, respectively. Fig. 12e reveals the repeated healing response of specimen reinforced by both PMMA/PAAm/epoxy and PMMA/PAAm/hardener tri-axial fibers.

In order to demonstrate the healing efficiency of each specimen, their normalized modulus values, defined as the ratio of flexural modulus of the specimen at each bending test cycle to flexural modulus at the first bending test, are compared as a function of healing cycles in Fig. 12f. All the normalized modulus values for each specimen have decreased with increasing bending/heal cycle number owing to damage accumulation in the structure associated the formation of new cracks as well as the growth or coalescence of old cracks in each bending test cycle. It is clearly seen from Fig. 12f that the specimens reinforced by PMMA/PAAm/DCPD tri-axial healing fibers with the mean fiber diameter of 200 nm experiences significantly lower reduction in normalized modulus per cycle than that reinforced by tri-axial hollow fibers. This result indicates that the presence of healing fibers inside the structure can trigger the healing reaction to repair the cracks and recover the mechanical properties of specimens to certain extent. On the other hand, specimens reinforced by PMMA/PAAm hollow fiber and PMMA/PAAm/DCPD healing fibers with average fiber diameter of 1 μm show similar reduction in normalized modulus up to the first healing cycle; however, upon increasing the cycle number, fibers including healing agent start to recover the mechanical properties of matrix and nearly retain normalized modulus of the composite after each bending/heal cycle while modulus values of specimens without healing ability decrease gradually in each cycle. Furthermore, the normalized modulus reduction in the first cycle for specimen reinforced by 1 μm DCPD healing fibers is higher than specimen reinforced by 200 nm healing fiber which is because of higher stress concentrations and in turn denser crack formation in specimens reinforced by larger fibers. However, the reduction in mechanical properties of matrix reinforced by healing fibers having a larger diameter reaches a stable value and subsequently does not change as a function of healing cycle which can be explained by excess amount of healing agent

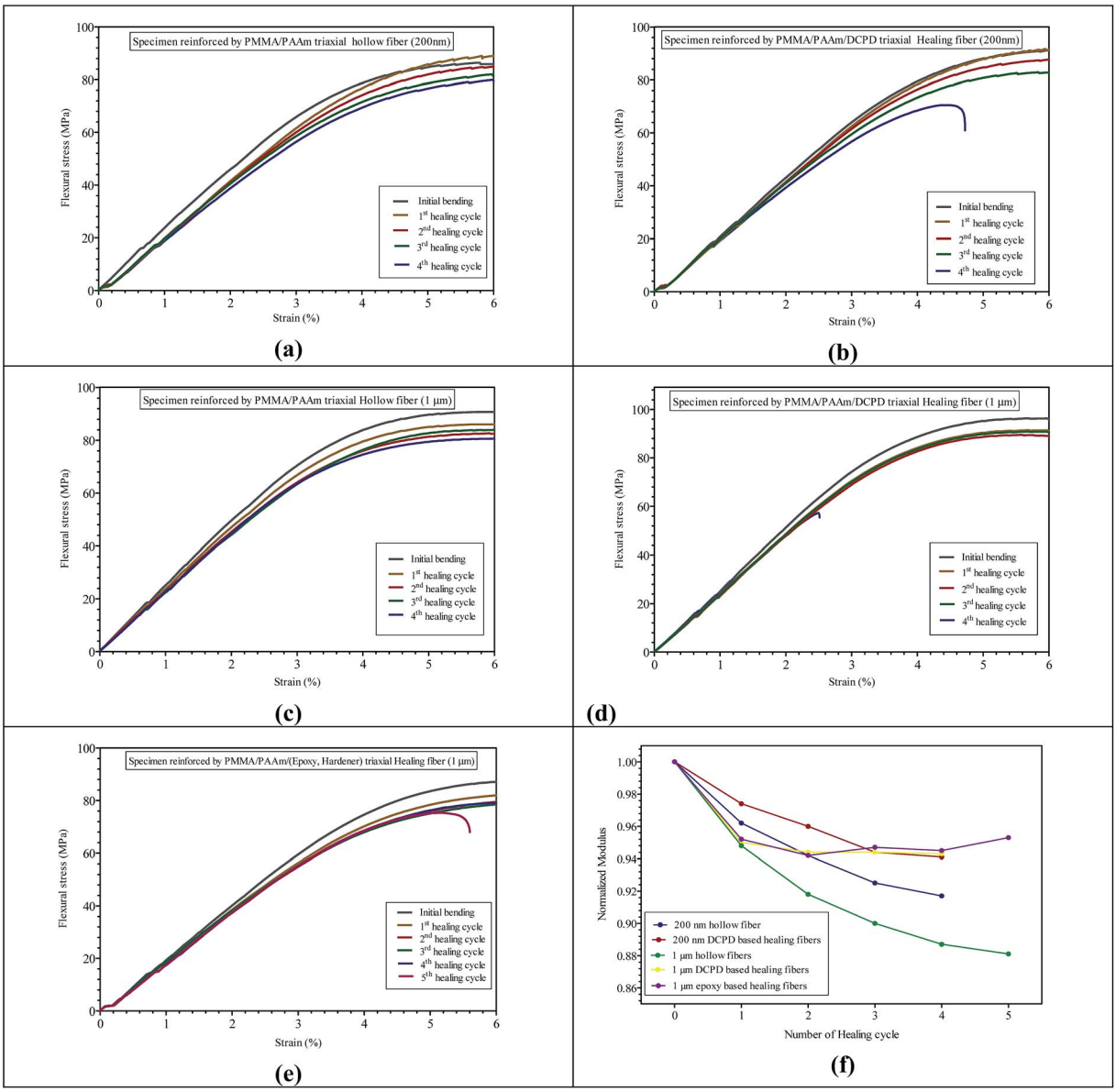

Fig. 12 Flexural stress–strain curves of specimens reinforced by (a) PMMA/PAAm tri-axial hollow fibers with the average diameter of 200 nm, (b) PMMA/PAAm/DCPD healing fibers with the average diameter of 200 nm, (c) PMMA/PAAm tri-axial hollow fibers with average diameter of 1 μm, (d) PMMA/PAAm/DCPD tri-axial healing fibers with the average diameter of 1 μm (e) PMMA/PAAm/(hardener, epoxy) tri-axial healing fibers with the average diameter of 1 μm and (f) normalized flexural modulus of composites reinforced by tri-axial hollow and healing fibers with different diameters as a function of healing cycle.

Table 1 Percent modulus reduction of specimens in each cycle based on initial modulus value

		200 nm hollow fibers	200 nm DCPD based healing fibers	1 μm hollow fibers	1 μm DCPD based healing fibers	1 μm epoxy and hardener based healing fibers
Modulus reduction (%)	1st cycle	96.2	97.4	94.79	95	95.2
	2nd cycle	94.2	95.95	91.78	94.4	94.2
	3rd cycle	92.5	94.37	89.9	94.4	94.7
	4th cycle	91.7	94.14	88.69	94.3	94.5
	5th cycle	—	—	88.1	—	95.3

encapsulated inside these kinds of fibers. This is further contributed by the higher amount of DCPD monomer inside larger diameter tri-axial fibers and the release of higher amount of healing agent into the crack area in each healing cycle.

In addition, the recovery for specimen with 200 nm fibers starts at the first cycle, but the reduction in normalized modulus gradually decreases with increasing cycle number since smaller healing fibers trigger the repairing mechanism effectively for nano and sub-micron scale cracks but the encapsulated healing agent is not enough to fill the cracks in micron scale. At this point, DCPD encapsulated tri-axial fibers having larger mean fiber diameter are much proper for healing process of micro cracks and fibers with finer diameter can heal nano-scale cracks efficiently. Moreover, epoxy matrix is concurrently reinforced by PMMA/PAAm/epoxy and PMMA/PAAm/hardener tri-axial fibers with the fiber diameter of 1 μm in order to measure and compare their self-healing efficiency with formerly introduced results. As seen from Fig. 12f, the healing degree of epoxy based healing system is slightly higher than DCPD based healing system. Epoxy based healing specimen does not fail at the 4th healing cycle whereas DCPD based healing systems prepared with 200 nm and 1 μm completely fail at this cycle. In addition, specimen reinforced by both tri-axial fibers including hardener and epoxy can heal itself until 5th healing cycle. Accordingly the differences in healing cycles with different healing agents can be attributed to the fact that the epoxy healing system shows higher compatibility with epoxy based matrix while healing material produced by ROMP of DCPD monomer in the presence of Grubbs' catalyst is not compatible with the surrounding matrix like epoxy based system and hence causes the stress concentration leading to the failure of specimens at 4th healing cycle. One can see from Table 1 that the percentage reduction in the modulus of epoxy-based specimen has leveled off indicating that the self healing process is active, effective, and hence able to preserve the mechanical properties of composite under high loadings.

Fracture surface characterization

Fig. 13 exhibits SEM images of the fracture surfaces of tri-axial fibers reinforced composites that are obtained at the end of 4th healing cycle. Fig. 13a corresponds to specimen reinforced by PMMA/PAAm hollow fiber with average diameter of 1 μm while Fig. 13b represents the fracture area of specimen with PMMA/PAAm/DCPD tri-axial healing fibers with average diameter of 1 μm. The fracture surface of specimen reinforced by hollow tri-axial fibers with the diameter of 1 μm looks very fragmented and rough. In addition, Fig. 13a reveals the severe crack formations induced by repeated bending tests on the specimen reinforced by hollow fibers on the composite structure. On the other hand, Fig. 13b represents the fracture surface of specimen reinforced by PMMA/PAAm/DCPD tri-axial healing fibers, and it can be seen clearly that new born polyDCPD films are formed by the release of encapsulated healing agent from the ruptured fibers into the cracked area and then reaction with pre-dispersed catalyst particles in outer layer of fibers. Therefore, the smooth surfaces are observed in the cross-sectional area of tri-axial healing fibers because healing agents filled and covered the damaged regions by the initiation of polymerization process. In the absence of healing agent, crack regions in the fracture area are seen clearly in Fig. 13a. However, in the presence of healing agent, the fracture surface has a smoother appearance due to polymerization of released DCPD monomer thereon as seen in Fig. 13b. This is the evidence for the efficient healing mechanisms and polymer coverage of crack regions. Fig. 13c shows specimens reinforced by PMMA/PAAm hollow fiber with average diameter of 200 nm while Fig. 13d exhibits the fracture area in the specimen with PMMA/PAAm/DCPD tri-axial healing fibers with average diameter of 200 nm. The fracture surface of specimen reinforced by tri-axial electrospun fiber with average fiber diameter of 200 nm in both case of hollow and healing fibers shows very smoother surface morphology than one of similar specimens reinforced by 1 μm fiber. However, size of the cracks on specimen reinforced by fibers with 200 nm are very small and thus limited amount of healing agents is released into the fracture area or inside the cracks and films of healing polymer occurred by healing process is not distinguishable in the SEM images but healing process has been already confirmed by mechanical tests after repetitive cycles. In addition, Fig. 13c and d exhibit very uniform distribution of fibers in the composite structure and nano scale holes on the surface of cracks can be seen clearly.

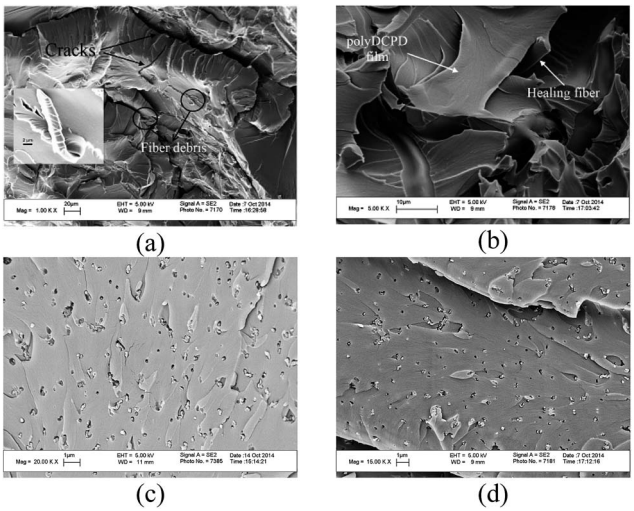

Fig. 13 SEM images of fracture area of (a) PMMA/PAAm tri-axial hollow fiber reinforced epoxy specimen with the fiber diameter of 1 μm, (b) PMMA/PAAm/DCPD tri-axial healing fiber reinforced epoxy specimen with the fiber diameter of 1 μm, (c) PMMA/PAAm tri-axial hollow fiber reinforced epoxy specimen with the fiber diameter of 200 nm (d) PMMA/PAAm/DCPD tri-axial healing fiber reinforced epoxy specimen with fiber diameter of below 200 nm.

Conclusions

Novel architecture of electrospun multi-walled healing fibers are utilized in order to encapsulate various healing agents with two different protective walls. For the first design of healing

fibers, DCPD as a healing agent is encapsulated inside the electrospun fibers with two different polymeric layers wherein the middle layer encapsulates healing agent due to its low affinity, and outer layer is compatible with epoxy matrix. The dispersion of metal catalysts into outer layer of fibers preserves the activity of catalyst during manufacturing process, reduces the required amount of catalyst in comparison to conventional catalyst dispersion into epoxy matrix, and provides the direct contact between the catalyst and healing monomer in crack region. The presence of an intermediate layer having low affinity to healing agents facilitate the encapsulation of healing agents with very high active nature such as amine based hardeners into polymeric shells. In the second design of self healing fibers, epoxy resin and amine-based curing agent are separately encapsulated in multi-axial electrospun fibers. The low affinity between the inner wall polymer and encapsulated healing agent within the core of fibers minimizes the environmental effect on healing agents and decreases the diffusion rate of healing agent through the wall of fiber hence extending the efficiency and lifetime of healing functionality of fibers. In addition, the effect of fiber diameter (nano or micron scale) and the type of self-healing agent (DCPD monomer and epoxy resin) on self-healing properties of the produced composites were investigated by comparing mechanical properties. It is shown that healing fibers with larger mean diameter are much more appropriate for healing micro cracks whereas fibers with finer diameter can heal nano-scale cracks more effectively. The healing efficiency of epoxy based healing system is observed to be slightly higher than DCPD based healing system given that epoxy based healing specimen has shown five successful healing cycles while DCPD based healing specimens were broken after the fourth cycle. The reduction in mechanical properties of matrix reinforced by healing fibers reaches a stable value and subsequently does not change as a function of healing cycle while normalized modulus of specimens reinforced by hollow fibers continuously decreases in each cycle. To reiterate, the unique structure of multi-walled electrospun fibers developed in this work has a high potential to create a novel self healing, smart and responsive materials with enhanced functionalities.

Acknowledgements

The authors gratefully acknowledge financial support from the Scientific and Technical Research Council of Turkey (TUBITAK) with the project numbers of 112M312/COST MP1202 and 112M357, and also thank to ESTEEM2 EU project for TEM characterization, Assoc. Prof. Cleva W. Ow-Yang for her help on Cathodoluminescence characterization and PhD student Omid Baghoojari for his help in rheological measurements.

References

1 A. Zucchelli, M. L. Focarete, C. Gualandi and S. Ramakrishna, *Polym. Adv. Technol.*, 2011, **22**, 339–349.
2 B. C. Ray and D. Rathore, *Polym. Compos.*, 2015, **36**, 410–423.
3 Y.-K. Song and C.-M. Chung, *Polym. Chem.*, 2013, **4**, 4940–4947.
4 J. W. C. Pang and I. P. Bond, *Compos. Sci. Technol.*, 2005, **65**, 1791–1799.
5 G. Williams, R. Trask and I. Bond, *Composites, Part A*, 2007, **38**, 1525–1532.
6 S. R. White, N. R. Sottos, P. H. Geubelle, J. S. Moore, M. R. Kessler, S. R. Sriram, E. N. Brown and S. Viswanathan, *Nature*, 2001, **409**, 794–797.
7 C. Dry, *Compos. Struct.*, 1996, **35**, 263–269.
8 D. G. Shchukin, *Polym. Chem.*, 2013, **4**, 4871–4877.
9 J. A. Syrett, C. R. Becer and D. M. Haddleton, *Polym. Chem.*, 2010, **1**, 978–987.
10 M. Motuku, U. K. Vaidya and G. M. Janowski, *Smart Mater. Struct.*, 1999, **8**, 623–638.
11 R. S. Trask, G. J. Williams and I. P. Bond, *J. R. Soc., Interface*, 2007, **4**, 363–371.
12 S. M. Bleay, C. B. Loader, V. J. Hawyes, L. Humberstone and P. T. Curtis, *Composites, Part A*, 2001, **32**, 1767–1776.
13 D. Y. Wu, S. Meure and D. Solomon, *Prog. Polym. Sci.*, 2008, **33**, 479–522.
14 S. Sinha-Ray, D. D. Pelot, Z. P. Zhou, A. Rahman, X. F. Wu and A. L. Yarin, *J. Mater. Chem.*, 2012, **22**, 9138–9146.
15 X. Xia, X. Wang, H. M. Zhou, X. Niu, L. G. Xue, X. W. Zhang and Q. F. Wei, *Electrochim. Acta*, 2014, **121**, 345–351.
16 Z. Sun, E. Zussman, A. L. Yarin, J. H. Wendorff and A. Greiner, *Adv. Mater.*, 2003, **15**, 1929–1932.
17 X.-F. Wu and A. L. Yarin, *J. Appl. Polym. Sci.*, 2013, **130**, 2225–2237.
18 M. W. Lee, S. An, C. Lee, M. Liou, A. L. Yarin and S. S. Yoon, *ACS Appl. Mater. Interfaces*, 2014, **6**, 10461–10468.
19 J. H. Park and P. V. Braun, *Adv. Mater.*, 2010, **22**, 496–499.
20 T. J. Mitchell and M. W. Keller, *Polym. Int.*, 2013, **62**, 860–866.
21 X. F. Wu, A. Rahman, Z. P. Zhou, D. D. Pelot, S. Sinha-Ray, B. Chen, S. Payne and A. L. Yarin, *J. Appl. Polym. Sci.*, 2013, **129**, 1383–1393.
22 S. Neuser and V. Michaud, *Polym. Chem.*, 2013, **4**, 4993–4999.
23 J. D. Rule, E. N. Brown, N. R. Sottos, S. R. White and J. S. Moore, *Adv. Mater.*, 2005, **17**, 205–208.
24 A. S. Jones, J. D. Rule, J. S. Moore, S. R. White and N. R. Sottos, *Chem. Mater.*, 2006, **18**, 1312–1317.
25 M. Majchrzak, P. J. Hine and E. Khosravi, *Polymer*, 2012, **53**, 5251–5257.
26 T. C. Mauldin, J. D. Rule, N. R. Sottos, S. R. White and J. S. Moore, *J. R. Soc., Interface*, 2007, **4**, 389–393.
27 D. F. Taber and K. J. Frankowski, *J. Org. Chem.*, 2003, **68**, 6047–6048.
28 L. Guadagno, P. Longo, M. Raimondo, C. Naddeo, A. Mariconda, A. Sorrentino, V. Vittoria, G. Iannuzzo and S. Russo, *J. Polym. Sci., Part B: Polym. Phys.*, 2010, **48**, 2413–2423.
29 B. Alcaide, P. Almendros and J. M. Alonso, *Chemistry*, 2003, **9**, 5793–5799.
30 Y. Tao, Z. Lin, R. Min Zhi and Z. Ming Qiu, *Smart Mater. Struct.*, 2008, **17**, 015019.
31 K. S. Toohey, C. J. Hansen, J. A. Lewis, S. R. White and N. R. Sottos, *Adv. Funct. Mater.*, 2009, **19**, 1399–1405.
32 Z. He and Y. Jinglei, *Smart Mater. Struct.*, 2014, **23**, 065003.

33 H. Zhang, P. Wang and J. Yang, *Compos. Sci. Technol.*, 2014, **94**, 23–29.
34 D. A. McIlroy, B. J. Blaiszik, M. M. Caruso, S. R. White, J. S. Moore and N. R. Sottos, *Macromolecules*, 2010, **43**, 1855–1859.
35 S. Khoee and Z. Kachoei, *RSC Adv.*, 2015, **5**, 21023–21032.
36 J. Seyyed Monfared Zanjani, B. Saner Okan, I. Letofsky-Papst, M. Yildiz and Y. Z. Menceloglu, *Eur. Polym. J.*, 2015, **62**, 66–76.
37 J. S. M. Zanjani, B. S. Okan, Y. Z. Menceloglu and M. Yildiz, *J. Reinf. Plast. Compos.*, 2015, **34**, 1273–1286.
38 M. R. Kessler and S. R. White, *Composites, Part A*, 2001, **32**, 683–699.
39 G. O. Wilson, M. M. Caruso, N. T. Reimer, S. R. White, N. R. Sottos and J. S. Moore, *Chem. Mater.*, 2008, **20**, 3288–3297.
40 L. Guadagno, P. Longo, M. Raimondo, C. Naddeo, A. Mariconda, V. Vittoria, G. Iannuzzo and S. Russo, *Composites, Part B*, 2011, **42**, 296–301.
41 M. M. Demir, N. Horzum, A. Tasdemirci, K. Turan and M. Guden, *ACS Appl. Mater. Interfaces*, 2014, **6**, 21901–21905.
42 J. Y. Shieh, H. J. Hwang, S. P. Yang and C. S. Wang, *J. Polym. Sci., Part A: Polym. Chem.*, 2005, **43**, 671–681.
43 K. Kaniappan and S. Latha, *Int. J. ChemTech Res.*, 2011, **3**, 708–717.
44 S. Ü. Çelik and A. Bozkurt, *Eur. Polym. J.*, 2008, **44**, 213–218.
45 R. Murugan, S. Mohan and A. Bigotto, *J. Korean Phys. Soc.*, 1998, **32**, 505–512.
46 L. Yuan, G. Liang, J. Xie, L. Li and J. Guo, *Polymer*, 2006, **47**, 5338–5349.
47 C. Liu, R. Bai and Q. San Ly, *Water Res.*, 2008, **42**, 1511–1522.
48 M. A. Khan, N. Haque, A. A. Kafi, M. N. Alam and M. Z. Abedin, *Polym.-Plast. Technol. Eng.*, 2006, **45**, 607–613.